Multi-nozzle electrospray method for high-throughput uniform superhydrophobic coating

Kye-Si Kwon (kskwon@sch.ac.kr)
Soonchunhyang University
Md. Abu Mosa
Soonchunhyang University
Se Hyun Kim
European University of Bangladesh

Research Article

Keywords: electrospray, multi-nozzle, crosstalk, uniformity of coated layer, drying process, superhydrophobic coating

Posted Date: February 7th, 2022

DOI: https://doi.org/10.21203/rs.3.rs-1304740/v1

Abstract

Electrospray is an effective method to fabricate functional layers on substrates. With electrospray, uniform and fine droplets can be created and attracted to the substrate without being blown away using the electric field formed by the nozzle and the substrate. The uniformity of coated layer is seldom affected by the fluid drying process (such as Marangoni flow on substrates) since the size of droplets could reach micron level and the solvents in the droplets could evaporate quickly. That is why the electrospray process is often referred to as 'dry deposition'. However, when a multi-nozzle electrospray system is considered for a faster fabrication process of large substrates, the drying process could be completely different from that of a single nozzle system. In addition, crosstalk and non-uniform spray volume from each nozzle could be an additional issue to be addressed. In this study, we proposed a multi-nozzle electrospray system and process to average out the non-uniformity of the spray amount and obtain the uniformity of the layer through a fast-drying process. Finally, we demonstrated the effectiveness of our proposed methods by fabricating superhydrophobic layers on a highly insulating substrate.

Introduction

Electrospray method is an effective coating method, which uses monodisperse charged micro-droplets. In an electrospray system, a high voltage is applied to a nozzle with a grounded substrate. Therefore, a highly charged ink droplet develops into atomization status by overcoming the surface tension of the liquid. The atomized droplets are attracted to the substrate due to the electrical field formed by a high voltage at the nozzle and grounded substrate. The liquid properties such as surface tension, viscosity, dielectric constant and electrical conductivity play a vital role in electrospray process. The operating parameters are flow rate, electrical field strength[1] and nozzle diameter[2]. Here, important parameters of electrospray method may be the flow rate and electric field. The electrospray atomization techniques have a wide range of applications in mass spectrometry[3], thin film deposition[4], painting[5] and bio-application[6].

Most of the research on electrospray has been based on the single nozzle configuration. The low deposition rate is one of the crucial drawbacks that have prevented possible industrial applications of this method. It can explain by scaling laws given by Loscertales et al.[7] and Gañan et al.[8]. These laws are related to flow rate and droplet size. According to these laws, if the desired particle size is small, the mass flow rate should be sufficiently reduced. As a result, electrospray uses a very low flow rate to generate fine droplets. Due to the low flow rate, the deposition process has been very slow. For high throughput coating, a multi-nozzle electrospray system must be used.

Several studies[9–16] have been published to increase the throughput using multi-nozzle electrospray. Parhizkar et al. investigated the performance of a multi-needle electrospray system for forming polymeric micro or nanoparticles[11]. They designed two different configurations for four nozzles based on either the linear or circular array. However, there are issues of non-equal spray behaviors of each nozzle. When a

liquid is supplied to nozzles, it can be charged by a high electrical potential applied to the nozzles. As a result, the liquid meniscus of the nozzle takes the form of a stable cone known as a Taylor cone. Jets spray is emitted from the apex of this cone. If the number of nozzles in a multi-nozzle system is increased, the space charge around the nozzle increases due to the clouds of charge droplets[15]. As a result, some of the menisci could lose their conical shape and, thereby, the cone jet behaviors may be different according to nozzle locations of the multi-spray system[17]. The electrical field interference (crosstalk) among neighboring nozzles can cause non-uniformity of spray deposition. In order to obtain uniform coated layers, it is necessary to ensure that all nozzles work in a steady cone-jet mode[16]. Some authors often suggest the use of additional extractor electrode[18–20] which is placed below the nozzle array. The droplets generated from the nozzle can pass through the aperture in the extractor. The extractor electrode reduces the electrostatic interference among the adjacent nozzles and electrically shields the Taylor cones from the spray cloud.

The deflection of the meniscus i.e., 'end effect'[12] at boundary nozzles is another limitation of multi-nozzle electrospray. Even though capillary nozzles in a multi-nozzle system have the same potential, they do not have the same electric field at the boundary nozzles[12]. The end effect arises from the asymmetric electric field at the tip of the nozzle and repulsive forces among the neighboring jet[12,13,21]. Several researchers[12–14,21] attempted to solve the problem by placing non-jetting nozzles (dummy nozzle) at the boundary of the array. No liquid is fed through the dummy nozzle, but the same potential is maintained, which reduces the end effect of the active nozzles by creating an external electric field around the end of the array.

In this research, we proposed a uniform and high-speed multi-nozzle electrospray method by overcoming previous problems of non-uniform deposition. We demonstrate the effectiveness of our proposed method by fabricating superhydrophobic layers on highly insulating substrates. There have been attempts to use the electrospray method for fabricating superhydrophobic layers. Wei Jia el. made a superhydrophobic membrane of PDMS-POSS nanocomposite on polyvinylidene fluoride (PVDF) substrate by electrospray method[22]. In their research, they showed that this method can produce nano-scaled surface roughness. Eun Kyeong et al. fabricated a highly rough fluorinated superhydrophobic silica layer on Si(100) substrates by electrospray method[23]. However, in case of highly insulating surfaces such as printed circuit boards (PCB) with the conductivity of 10^{-20} S m^{-1} as well as other plastic substrates (polyethylene terephthalate (PET) with conductivity 10^{-21} S m^{-1} and polyimide (PI) with conductivity 10^{-15} S m^{-1}), the electrospray deposition methods have been unsuccessful. The main difficulties result from the repulsive force of the deposited charged layer against the incoming charged droplets[24–26]. As a result, the deposition efficiency has been very low because most of the incoming droplets could be deposited on the outside of the substrate[27]. To solve this issue, our group developed a new electrospray method based on AC voltage on the substrate to fabricate superhydrophobic coatings on PCB substrate based on a single nozzle configuration[27]. The AC voltage increased the movement of the electrostatic charges, assisting the charge redistribution on the insulating surface resulting in effective spray deposition[28,29]. However, our previous work was performed by using a single nozzle for the deposition. Considerable time has been

required for the deposition because electrospray deposition has problems of slow deposition rate. For example, 600 s was required for deposition of 0.6 μm thickness of a superhydrophobic layer on a target location[30].

Here, we extended our previous study of AC based electrospray method by using a multi-nozzle for high throughput fabrication of superhydrophobic surfaces. For this purpose, we have used five nozzles with inter nozzle spacing of 12 mm. Since the nozzle-to-nozzle distance is not sufficiently far, we observed significant crosstalk behaviors and the deposition amount was different according to nozzles. To average out the deposition amount, we proposed the zig-zag relative motion of nozzles with respect to the substrate. For practical applications, a sufficient amount of materials should be deposited in order to ensure the reliability of the coated layer. Unlike single nozzle deposition, a large amount of sprayed materials can be deposited within a short period without proper solvent evaporation on substrates. This will cause additional problems of non-uniform layer thickness caused by drying process. In this work, we propose the use of a hot blower for faster solvent evaporation and curing of the deposited material. Optimal conditions for the hot blower are important as it should provide sufficient airflow and heat for faster evaporation, but the airflow should not blow the spray droplets away during flight. By fabricating superhydrophobic layers, we demonstrated that the quality of deposition layers could be improved by optimizing drying conditions.

Results And Discussion

Atomization process in electrospray deposition

In electrospray deposition process, a single Taylor cone-jet shaped meniscus forms by stabilizing electrostatic repulsion and surface tension[31]. If the applied voltage at the nozzle is high enough to produce electrostatic repulsive force within charged droplets, the liquid breaks up into finer charge droplets by overcoming the surface tension[32]. The atomization process can go through several steps. The primary charge droplets produced by a Taylor cone, shrink due to the evaporation of the solvent. The shrinkage process continues until the droplet radius approaches the Rayleigh limit[33]. Rayleigh limit describes the stability limit of a charged droplet, which is affected by the opposing forces of the surface tension and electrostatic repulsive force. Droplets in conditions close to the Rayleigh limit are unstable and can undergo Coulomb fission. The charge in the droplets at this limit can be expressed by the critical radius of the droplets as:

$$q_R = 8\pi \left(\gamma \epsilon_o r^3\right)^{1/2} \qquad (1)$$

where, r, q_R, γ and ϵ_o are the radius of the droplets, the total charge on the droplet, surface tension of the liquid and electrical permittivity of the liquid, respectively. The diameter of the atomized droplet could be less than 10 μm having normal distribution behavior[34]. The energy required for droplet evaporation

comes from the thermal energy of the ambient air. Due to the evaporation, droplet size decreases while the same amount of charges remains. As a result, the charge density of the droplet increases until the electrostatic repulsive force within the droplet overcomes the surface tension. At this point, the droplets are no longer stable, which is called Rayleigh instability. Then the droplets (parent droplets) experience Coulomb fission and release new droplets (child droplets) with a small amount of mass (around 2% of the parent droplet) and a greater charge density (about 15% of the parent droplet)[35]. The process of evaporation and fission is repeated by both parent and child droplets until reaching the substrate.

The spray deposition process could be affected by the accumulated charges of deposited materials on highly insulating substrate[36,37]. Recently, this issue was solved by applying AC voltage on substrate[27]. The AC voltage is effective for all substrates regardless of the conductivity[27]. In this research of multi-nozzle electrospray application, we applied AC voltage at the substrate to enhance the deposition efficiency.

Crosstalk and end effects of multi-nozzle electrospray

The electric field interference among neighboring nozzles, i.e., crosstalk effect, depends mainly on the distance between nozzles, when flow rate/pressure, voltage and nozzle inner diameter are constant[10]. In this section, we investigated the effect of the crosstalk using two nozzles with a distance adjustor, as shown in Figure 1. The nozzle-to-nozzle distance varied from 1 cm to 5 cm and the inner diameter of the nozzle was 330 μm. A detailed discussion on crosstalk effects is provided in the supplementary information (Section S1).

Figure 2(a-d) shows the electrospray behaviors of two nozzles with different nozzle spacing. Here, no significant crosstalk effects could be observed in the deposited shape when two nozzles were used. However, when we used a five-nozzle spray-head with a nozzle-to-nozzle distance of 1.2 cm, we could observe the crosstalk effects from the deposition shape as shown in Figure 2(e). In the case of a multi-nozzle spray head, having more than three nozzles, the cone jets could be deflected in different ways due to the end effects[12]. The end effect arises from asymmetric electric field in the boundary nozzles. The spray behavior of nozzles in the middle shows that the spray process was more stable and could result in more uniform coated results than that of the nozzles on both ends. Figure 3 helps to explain this phenomenon, which illustrates electrospray behaviors caused by the asymmetric electric field at the tip of the nozzles. The electric field at various points (A, B & C) in a nozzle, as shown in Figure 3(a), could be different according to nozzle configuration[10,12]. As illustrated in Figures 3(b) and (c), the spray emits from the point where the electric field is the strongest. In case of a linear array with five nozzles, the electric field is the highest at both ends[10] (Point A in case of nozzle 1 and point C in case of nozzle 5). As a result, the spray jet from the edge nozzles (nozzles 1 and 5) deflected from the capillary axis. Also, the charged spray droplets in flight from a specific nozzle produce repulsive forces to sprayed droplets from neighboring nozzles. As a result, when multiple nozzles are used for electrospray deposition, the deposition layer may not be uniform over the entire area of the substrate.

Uniform deposition method based on motion control

As discussed in the previous section, non-uniform deposition areas from each nozzle have resulted from crosstalk and the end effect. Additionally, the sprayed substrate contains a non-sprayed region between two nozzles if the scanning movement is not intended to overlap. To increase the uniformity of deposition layers, we proposed ‘zig-zag’ relative motion of spray head with respect to the substrate (Refer to the experimental section). The zig-zag motion could increase the thickness uniformity of coated layers by averaging out non-uniform spray jetting from each nozzle. The scanning speed of motion movement can affect the deposition amount on substrates. For example, there can be acceleration and deceleration when motion direction changes. So, the deposition area should be sufficiently large compared to the substrate, such that scanning speed passing through the substrate should be constant.

Drying optimization for uniform layer thickness

For better deposition of materials, the surface energy of the PCB substrates was improved by (Ar and O_2 mixed, radio frequency (RF) driven atmospheric pressure plasma) plasma treatment prior to electrospray (Supplementary information, Movie S1). By combining Ar and O_2, RF-generated plasma can increase the substrate wettability and adhesion qualities[38,39]. The detailed plasma pre-treatment effects are discussed in the supplementary information (Section S2).

Even if the plasma treatment could improve surface conditions by improving adhesion properties of the substrate, the surface as well as the thickness of the dried coating layer, is not uniform. The uniformity is affected by the evaporation process. The non-uniformity becomes more severe in the case of multi-nozzle spray deposition since a significant amount of materials could be deposited with non-evaporated solvents in it. The evaporation rate depends on the spray parameters such as droplet sizes and stand of distances, environmental conditions such as temperature and relative humidity and ink formulation parameters such as solute concentration and solvent volatility[40]. The solvent volatility is one of the most important properties which influence the evaporation rate and the ultimate particle morphology[41]. The severe agglomeration of particles on the substrate can avoid by immediate evaporation of the solvents[40]. In the case of a single nozzle electrospray system, evaporation issue rarely causes a problem since the solvent atmosphere is not so dense and the deposition rate is relatively low. However, when the deposition rate is increased by employing multi-nozzle electrospray, the solvent atmosphere could be dense, resulting in a slower evaporation rate. In this case, the ambient atmosphere is unable to supply adequate energy for the evaporation of solvents in a large number of deposited droplets. As a result, the deposited materials with unevaporated solvents could coalesce on the surface, as shown in Figure 4(a). This effect creates severe non-uniformity of the coated layer, as shown in Figure 4(b). The coalescence of the droplets in-flight along their trajectory towards the substrate is extremely rare because charged droplets repel one another. Rather, it occurs right after deposition on substrates. In conventional inkjet application, a substrate (platen) heater is often considered to expedite the solvent evaporation of deposited materials[42]. In our present case of using the multi-nozzle spray system, the platen heater has limitations of improving the uniformity of layer, as shown in Figure 4(c). Furthermore, the cured coated layer did not show sufficient hydrophobic characteristics having a contact angle of only 131˚.

To improve the uniformity of the coating by accelerating solvent evaporation, a hot blower (STEL670, STANLEY, USA) was integrated into the spray system. An airflow duct was designed to effectively supply hot air to the substrate, as shown in Figures 5(a-d). Photos of the hot blower and the flow duct are presented in the supplementary information (Section S3). The use of the hot blower has the further benefit of in-situ curing during the deposition without requiring an additional curing process.

Two different configurations were investigated to optimize the drying process using the hot blower. The first configuration was based on two independent operations for spraying and drying. Figures 5(a) and (b) shows hardware configuration based on separate drying unit. We investigated optimum temperature and wind speed using this configuration. In this case, right after printing the spray deposition pattern (zig-zag motion) once, the substrate travels to the location where the hot blower is positioned for the solvent evaporation and curing of deposited materials. The process of spraying and drying is repeated multiple times to increase the thickness of the coated layer. However, it could have limitation since there was a time delay in the drying process.

The second configuration uses a combined unit of spraying and drying, as shown in Figures 5(c) and (d). This configuration allows simultaneous deposition and evaporation process with a minimal time delay. In this case, the optimum conditions of the hot blower found in the first configuration are used for drying the deposited materials. The distance (D) between the nozzle head and the hot blower is important in this case, as the hot blower close to the nozzle head can blow away the spray droplets in flight. The effect of the distance on deposition quality is discussed later.

To understand the effect of substrate temperature on coating performance using the first configuration, a forward-looking infrared camera (E6390, FLIR, Sweden) was used to measure the temperature of the substrates according to different power (Level 1 to Level 4) of the hot blower. The wind speed at the outlet of the airflow duct was measured by using a typical anemometer (ST-111, Sincon, South Korea) based on the wind levels (Level 1 and Level 2) of the hot blower. Table 1 shows the temperature of the PCB substrate according to the heating levels and wind speeds of the hot blower when the hot blower was located 5 mm above substrates.

Table 1
Temperature of the PCB substrate at various heating levels (temperature at the outlet of the hot blower) and wind speeds, measured using FLIR camera.

	Temperature of the substrate (°C)			
Wind speed (m/s)	Leve 1 (100˚C)	Level 2 (150˚C)	Level 3 (200˚C)	Level 4 (250˚C)
1.5 (Level 1)	39.3	48.0	76.2	102.0
3.6 (Level 2)	47.7	62.0	98.8	150.0

The proper drying process is important in order to ensure coated layer uniformity. Figure 6(a) shows surface conditions of PCB substrate right after spray deposition using a zig-zag pattern five times. Figure

6(b) shows the contact angles of coated layers on the substrates. Here, all the conditions for spray deposition were the same except hot blower parameters such as power and wind speed. Note that the temperatures of the hot blower and substrate can be increased according to the power of the hot blower, as shown in Table 1. When the blower power was minimum (Level 1), the temperature of the substrates was measured to be around 50℃. On the other hand, the substrate temperature can be increased to 150℃ by maximizing the power (Level 4), which is close to the boiling point (170℃) of the solvent, 2-butoxy ethanol. In case of the substrate temperature could increase more than 150℃, additional post-processing of curing is unnecessary.

To ensure the curing of the deposited layers, the coated substrates were placed on a hot plate at 170℃ for 30 minutes. Figure 6(b) shows the water contact angles of the silica-coated substrates according to the temperatures of the substrate and wind speed at the outlet of the flow duct. The contact angles were different according to drying conditions. The contact angles increased according to the temperature as well as the wind speed. The coated layer using the maximum power of the hot blower and with a wind speed of 3.6 m/s showed superhydrophobic characteristics with a contact angle of 151°. However, heating alone without proper airflow could not make superhydrophobic layers when multi-nozzle was used.

The second configuration, in which the hot blower attached to the electrospray head, is used for drying the deposited materials instantly. However, if the distance between the electrospray head and the hot blower becomes too close, the hot blower can create adverse airflow that can affect the deposition by flying away droplets in flight. Thus, the distance between the multi-nozzle head and the hot blower can affect deposition quality, which can measure from the contact angle of the coated layer. To investigate the effect, we developed an experimental setup to adjust the distance (D) between the nozzle head and the hot blower, as shown in Figures 5(c) and (d). Refer to the video in the supporting material (Movie S2) for a better understanding. Figure 7 shows the water contact angle variation with the distance between the nozzles and the hot blower. As shown in Figure 7, the hot blower should locate more than 90 mm from the spray nozzle in order to ensure supper-hydrophobicity of the coated layer. The videos in the supporting material (Movie S3, Movie S4 & Movie S5) refer to observing the uniform superhydrophobic characteristics.

Characterization of deposited layer

The deposited silica layer could have micro/nano hierarchical roughness, which leads to hydrophobicity by reducing the contact area between water droplets and the solid surface[43,44] For better understanding of the microscopic structure, the characterization of surface roughness was carried out by using atomic force microscopy (AFM). Refer to the details in the supplementary information (Section S4). The root mean square surface roughness (R_{RMS}) of the coated layers was in the range of 80 nm to 100 nm. Note that the original (uncoated) PCB substrate had a surface roughness of 11.03 nm.

Sufficient thickness of the coated layer is important in order to ensure the reliability of the layer in presence of mechanical harshness. However, in case of using plastic substrates including PCB

substrates, it was very difficult to measure the thickness of the coated layers. To roughly understand layer thickness, we used glass substrate for fabricating superhydrophobic layers with the same conditions for multi-spray deposition discussed earlier. The contact angle of the coated glass substrate was 154 ° . The thickness of the coated layers on glass could easily be measured by using a 3-D profiler and FIB-SEM, as shown in Figure 8(a) and Figure 8(b). For thickness measurement using the 3D profiler, a part of the coated layer was removed by a knife, as shown in Figure 10(e). By using the conventional electrospray method, the thickness of the coated layer on glass substrate was only 0.87 μm[27]. When an alternating current voltage is applied to the substrate in a single nozzle deposition system, the thickness was measured to be 1.91 μm[27]. By implementing a multi-nozzle system, the coating layer thickness was further increased to 2.85 μm in the present method. It took 60 s to achieve this thickness of 2.85 μm over $5cm \times 5cm$ region of the PCB, while the previous method using the single nozzle takes the same amount of time to achieve a thickness of 1.91 μm on a single spot with a diameter of 4 cm[27]. The improvement in the deposition efficiency is due to the combined effect of AC voltage on the substrate holder and multi-nozzle deposition with a hot blower.

To investigate the reliability of coated layers, we performed the mechanical and chemical tests by using sandpaper abrasion and chemical attack (HCl), respectively. Even after the sandpaper abrasion (refer to Materials and Methods), the water contact angle was measured to be 147 ° , which indicates that the hydrophobicity of the surface remained almost the same as the original contact angle of 152 ° . For chemical attack, the superhydrophobic PCB substrate was submerged in 0.1 M HCL for 5 minutes (Supplementary information, Movie S7). There was no rapid chemical reaction when the coated substrate was immersed in HCL acid. The contact angle after the chemical test was measured 149 ° . The FE-SEM image of the surface before and after abrasion and chemical test is shown in Figure 9. There is no significant change in the surface morphology of the coating after the sandpaper abrasion and HCL submersion tests.

Concluding Remarks

We discussed two major issues of using multi-nozzles for electrospray: crosstalk and evaporation of deposited materials. In case of deposition using two nozzles, the two deposition areas appeared to be uniform if the nozzle to nozzle distance was as close as 1 cm. In case of electrospray deposition using more than three nozzles, the non-uniformity of jetting was unavoidable due to so-called ‘end effect’. However, the non-uniformity due to crosstalk did not lead to coated layer non-uniformity only if the zig-zag motion was used. In our experiment, simple vector motion with an angle of ±20° (zig-zag) was used. Nonetheless, the quality of the layers could not be improved and the layer did not show super-hydrophobicity without a proper drying process. Also, we found that the sufficient contact angle could not be achieved by using substrate heating only when the amount of solvents to evaporate is large. To solve the issue, we showed that the use of a hot blower was effective. Here, the heating and wind speed were both important. Especially by increasing wind speed from 1.5 ms^{-1} to 3.6 ms^{-1}, the contact angle could be significantly increased from 138° to 151°.

Our proposed method can be extended to electrospray deposition with more nozzles and has advantages over previous methods because it does not require dummy nozzles or extractors in order to achieve the desired coating quality.

Materials And Methods

Materials

Fumed silica nanoparticles (Aerosil R 972) with an average particle size of 16 nm was kindly donated from Evonic Industry, Germany. The epoxy resin (poly bisphenol A-co-epichlorohydrin), curing agent (4,4´-methhylenebis 2-chloroaniline) and reagent (2-butoxyethanol) were purchased from Sigma Aldrich, South Korea. First, an epoxy resin solution was made by mixing 0.5 g of epoxy resin (in pellet form) and 0.08 g of curing agent with 9.42 g of 2-butoxyehtanol for 8 hours at 70℃ using a magnetic stirrer. Secondly, a silica solution was made by stirring 0.45 g of fumed silica with 9.55 g of 2-butoxyethanol for 2 hours at room temperature with a magnetic stirrer. Finally, the epoxy resin solution (50% volume) and silica solution (50% volume) were mixed for 1 hour at room temperature with a magnetic stirrer. After mixing the hydrophobic coating solution, it was sonicated for five minutes. Our formulated solution has a silica content of 22.5 mg/L. The spray solution has a viscosity of 11 cP and surface tension of 23.17 mN/m were measured by a viscometer (DV III, Brookfield, USA) and a surface tension analyzer (SEO-DST30M, Kromtek, Malaysia), respectively. In our current study, we fabricated superhydrophobic coating on PCB substrates (FR-4, Sungsim Tech, South Korea) with a dimension of 5 cm × 5 cm.

Experimental Process for Multi-nozzle Electrospray for Superhydrophobic coating

A schematic diagram of experimental setup is illustrated in Figure 10(a). Figure 10(c) shows a multi-nozzle electrospray head, which was used for the electrospray deposition. Plastic nozzles (23G) with an inner diameter of 330 μm and an outer diameter of 640 μm were used for multi-nozzle electrospray deposition. Prior to the electrospray, the substrate surfaces were treated with RF-driven (argon+ oxygen) plasma (REX-300, RF Power Tech, South Korea) using the power 180 W. The Ar and O_2 discharge flow rates were 7 slpm (standard liter per minute) and 10 sccm (standard cubic centimeter per minute), respectively. The scanning speed of plasma treatment was set to 5 mm/s, while the distance between the plasma head and substrate was 3 mm. The spray deposition process was performed right after the plasma treatment of the substrate surface. A pressure regulator (Ultimus-I, Nordson EFD, USA) was used to apply 4 kPa of air pressure to the syringe barrel in order to push the deposition materials to each nozzle. It is important to keep the air pressure low enough to avoid big droplets dripping from the nozzles. Note that the air bubbles within the system (syringe, nozzle-head and nozzle) should be carefully eliminated since electrospray process became unstable when air bubbles are entrapped in the spray head.

A power supply (SHV30R, Conver Tech, South Korea) was used to apply a high DC voltage of 8 kV to the multi-head nozzle. The substrate holder was connected to AC voltage with a peak-to-peak amplitude of 1.6 kV and a frequency of 3 kHz in order to increase the deposition efficiency. For this purpose, AC signal was generated by using a function generator (Agilent 33220A, Agilent Technologies, USA) and then it was amplified by using a high voltage amplifier (2220m, Trek, USA). A stand-off distance of 5 cm between the nozzle tip and the substrate (collector) was maintained during the deposition process. A relative zig-zag motion of the multi-head nozzle with respect to the substrate was used to achieve uniform deposition throughout the whole surface of the substrate, as shown in Figure 10(d). The zig-zag relative motion of the spray head was generated with an angle of 20° between two tracing paths as shown in Figure 10(d). The vector speed of the motion was 150 mm/s. During spraying, a hot blower was used to minimize the solvent atmosphere and accelerate the evaporation of solvents in deposited materials on substrates.

The photo of experimental setup for electrospray deposition using multi-nozzles is shown in Figure 10(b).

Characterization of deposited layers

The water contact angle (CA) was measured to assess the hydrophobicity of the coated layers. An optical contact angle meter (Phoenix 300 Touch, SEO, South Korea) was utilized to measure the contact angles of prepared samples. Water contact angle (CA) measurement was performed at room temperature utilizing sessile drop method. The contact angle was obtained by dropping 8 µL of deionized water. The measurement process was repeated five times at different places on the substrate. Atomic force microscopy (AFM) (SPM 9700, Shimadzu, Japan) was used to assess the surface roughness of the platinum-coated samples. The surface roughness of the specified scan area (5µm × $5\mu m$)was determined in terms of the root means square roughness (R_{RMS}). A 3D profiler (ET 200, Kosaka Laboratory Ltd. Japan) was used to measure the thickness of the coated layer as shown in Figure 10(e). The layer thickness was also verified using the cross-sectional FIB-SEM (Lyra 3, TESCAN, Czech Republic).

Reliability test

Sandpaper abrasion and chemical attack using HCl were performed to assess the durability of the coated layer. For the mechanical test, the coated layers were dragged against a 1000 grit sandpaper with a 100 g load (Supplementary information, Movie S6). The specimen with the load was moved 5 cm by changing the direction of the motion and the movement cycle repeated 5 times. For the chemical test, the PCB substrate with coated layer was submerged in 0.1 M HCL for 5 minutes (Supplementary information, Movie S7). Surface morphologies of the coated layer before and after chemical and sandpaper test were investigated utilizing a field emission scanning electron microscope, FE-SEM (MIRA2, TESCAN, Czech Republic).

Declarations

Acknowledgement

This work was supported by the Technology Development Program of MSS [S2931106]. Kye-Si Kwon acknowledges the support from BK21 FOUR (Fostering Outstanding Universities for Research) (No. 5199991614564) and partial support from the Soonchunhyang University Research Fund.

Author Contributions

M. A. M. performed the experiment and prepared the manuscript. K.S.H performed the experiment. K.-S. K. supervised the whole experimental work and prepared the manuscript.

Conflict of interests

Authors declare no competing interests.

References

1. Gañán-Calvo, A. M. Cone-jet analytical extension of Taylor's electrostatic solution and the asymptotic universal scaling laws in electrospraying. *Phys. Rev. Lett.* **79**, 217–220 (1997).
2. Cloupeau, M. & Prunet-Foch, B. Electrostatic spraying of liquids in cone-jet mode. *J. Electrostat.* **22**, 135–159 (1989).
3. Griss, P., Melin, J., Sjödahl, J., Roeraade, J. & Stemme, G. Development of micromachined hollow tips for protein analysis based on nanoelectrospray ionization mass spectrometry. *J. Micromechanics Microengineering* **12**, 682 (2002).
4. Jaworek, A. Micro- and nanoparticle production by electrospraying. *Powder Technol.* **176**, 18–35 (2007).
5. Domnick, J. & Ye, Q. The Electrostatic Spray Painting Process with High-Speed Rotary Bell Atomizers : Influences of operating conditions and target geometries. in *9th Int. Conference on Liquid Atomization and Spray Systems* 11 (2003).
6. Li, X., Huang, J. & Edirisinghe, M. J. Novel patterning of nano-bioceramics: Template-assisted electrohydrodynamic atomization spraying. *J. R. Soc. Interface* **15**, 253–257 (2008).
7. De la Mora, J. F. & Loscertales, I. G. The current emitted by highly conducting Taylor cones. *J. Fluid Mech.* **260**, 155–184 (1994).
8. Gañán-Calvo, A. M., Dávila, J. & Barrero, A. Current and droplet size in the electrospraying of liquids. Scaling laws. *J. Aerosol Sci.* **28**, 249–275 (1997).
9. Lin, L. *et al.* Bio-inspired hierarchical macromolecule-nanoclay hydrogels for robust underwater superoleophobicity. *Adv. Mater.* **22**, 4826–4830 (2010).
10. Choi, K. H., Rahman, K., Khan, A. & Kim, D. S. Cross-talk effect in electrostatic based capillary array nozzles. *J. Mech. Sci. Technol.* **25**, 3053–3062 (2011).

11. Parhizkar, M. *et al.* Performance of novel high throughput multi electrospray systems for forming of polymeric micro/nanoparticles. *Mater. Des.* **126**, 73–84 (2017).
12. Rulison, A. J. & Flagan, R. C. Scale-up of electrospray atomization using linear arrays of Taylor cones. *Rev. Sci. Instrum.* **64**, 683–686 (1993).
13. Quang Tran, S. B. *et al.* Polymer-based electrospray device with multiple nozzles to minimize end effect phenomenon. *J. Electrostat.* **68**, 138–144 (2010).
14. Lojewski, B., Yang, W., Duan, H., Xu, C. & Deng, W. Design, fabrication, and characterization of linear multiplexed electrospray atomizers micro-machined from metal and polymers. *Aerosol Sci. Technol.* **47**, 146–152 (2013).
15. Bocanegra, R., Galán, D., Márquez, M., Loscertales, I. G. & Barrero, A. Multiple electrosprays emitted from an array of holes. *J. Aerosol Sci.* **36**, 1387–1399 (2005).
16. Duby, M. H., Deng, W., Kim, K., Gomez, T. & Gomez, A. Stabilization of monodisperse electrosprays in the multi-jet mode via electric field enhancement. *J. Aerosol Sci.* **37**, 306–322 (2006).
17. Oh, H., Kim, K. & Kim, S. Characterization of deposition patterns produced by twin-nozzle electrospray. *J. Aerosol Sci.* **39**, 801–813 (2008).
18. Almería, B., Deng, W., Fahmy, T. M. & Gomez, A. Controlling the morphology of electrospray-generated PLGA microparticles for drug delivery. *J. Colloid Interface Sci.* **343**, 125–133 (2010).
19. Deng, W. & Gomez, A. Influence of space charge on the scale-up of multiplexed electrosprays. *J. Aerosol Sci.* **38**, 1062–1078 (2007).
20. Lenguito, G., Fernandez Garcia, J., Fernandez de la Mora, J. & Gomez, A. Multiplexed Electrospray for Space Propulsion Applications. in *Proceedings of 46th AIAA Joint Propulsion Conference, AIAA* 6521 (2010). doi:10.2514/6.2010-6521.
21. Tang, K. & Gomez, A. On the structure of an electrostatic spray of monodisperse droplets. *Phys. Fluids* **6**, 2317–2332 (1994).
22. Jia, W. *et al.* Superhydrophobic membrane by hierarchically structured PDMS-POSS electrospray coating with cauliflower-shaped beads for enhanced MD performance. *J. Memb. Sci.* **597**, 117638 (2020).
23. Kim, E. K., Lee, C. S. & Kim, S. S. Superhydrophobicity of electrospray-synthesized fluorinated silica layers. *J. Colloid Interface Sci.* **368**, 599–602 (2012).
24. Park, J. & Hwang, J. Fabrication of a flexible Ag-grid transparent electrode using ac based electrohydrodynamic Jet printing. *J. Phys. D. Appl. Phys.* **47**, 405102 (2014).
25. Wei, C. *et al.* High-resolution ac-pulse modulated electrohydrodynamic jet printing on highly insulating substrates. *J. Micromechanics Microengineering* **24**, 45010 (2014).
26. Kim, B., Kim, I., Joo, S. W. & Lim, G. Electrohydrodynamic repulsion of droplets falling on an insulating substrate in an electric field. *Appl. Phys. Lett.* **95**, 204106 (2009).
27. Rahman, M. K. *et al.* High-Efficiency Electrospray Deposition Method for Nonconductive Substrates: Applications of Superhydrophobic Coatings. *ACS Appl. Mater. Interfaces* **29**, 182–190 (2021).

28. Manju, M. B., Vignesh, S., Nikhil, K. S., Sharaj, A. P. & Murthy, M. Electrical Conductivity Studies of Glass Fiber Reinforced Polymer Composites. *Mater. Today Proc.* **5**, 3229–3236 (2018).
29. Panteny, S., Stevens, R. & Bowen, C. R. The frequency dependent permittivity and AC conductivity of random electrical networks. *Ferroelectrics* **317**, 199–208 (2005).
30. Yoon, H. *et al.* A highly transparent self-cleaning superhydrophobic surface by organosilane-coated alumina particles deposited via electrospraying. *J. Mater. Chem. A* **3**, 11403–11410 (2015).
31. Disintegration of water drops in an electric field. *Proc. R. Soc. London. Ser. A. Math. Phys. Sci.* **280**, 383–397 (1964).
32. Gao, J. & Austin, D. E. Mechanistic Investigation of Charge Separation in Electrospray Ionization using Microparticles to Record Droplet Charge State. *J. Am. Soc. Mass Spectrom.* **31**, 2044–2052 (2020).
33. Rayleigh, Lord. XX. On the equilibrium of liquid conducting masses charged with electricity. *London, Edinburgh, Dublin Philos. Mag. J. Sci.* **14**, 184–186 (1882).
34. Sharma, B., Takamura, Y., Shimoda, T. & Biyani, M. A bulk sub-femtoliter in vitro compartmentalization system using super-fine electrosprays. *Sci. Rep.* **6**, 26257 (2016).
35. Merrill, M. H. Large-scale electrospray ionization methods for nanocoating application. in *ASME International Mechanical Engineering Congress and Exposition, Proceedings (IMECE)* 177–186 (2010). doi:10.1115/IMECE2010-38799.
36. Zhu, Y. & Chiarot, P. R. Surface charge accumulation and decay in electrospray printing. *J. Phys. D. Appl. Phys.* **54**, 75301 (2021).
37. Lei, L. *et al.* Obtaining Thickness-Limited Electrospray Deposition for 3D Coating. *ACS Appl. Mater. Interfaces* **10**, 11175–11188 (2018).
38. Kaynak, A., Mehmood, T., Dai, X. J., Magniez, K. & Kouzani, A. Study of radio frequency plasma treatment of PVDF film using Ar, O2 and (Ar + O2) gases for improved polypyrrole adhesion. *Materials (Basel).* **6**, 3482–3493 (2013).
39. Asghar, A. H. & Galaly, A. R. The effect of oxygen admixture with argon discharges on the impact parameters of atmospheric pressure plasma jet characteristics. *Appl. Sci.* **11**, 6870 (2021).
40. Boel, E. *et al.* Unraveling particle formation: From single droplet drying to spray drying and electrospraying. *Pharmaceutics* **12**, 625–682 (2020).
41. Sadek, C. *et al.* Drying of a single droplet to investigate process–structure–function relationships: a review. *Dairy Sci. Technol.* **95**, 771–794 (2015).
42. Kwon, K. S. *et al.* Review of digital printing technologies for electronic materials. *Flex. Print. Electron.* **5**, 43003 (2020).
43. Zhi, D., Lu, Y., Sathasivam, S., Parkin, I. P. & Zhang, X. Large-scale fabrication of translucent and repairable superhydrophobic spray coatings with remarkable mechanical, chemical durability and UV resistance. *J. Mater. Chem. A* **5**, 10622–10631 (2017).

44. Guo, Z., Liu, W. & Su, B. L. Superhydrophobic surfaces: From natural to biomimetic to functional. *J. Colloid Interface Sci.* **353**, 335–55 (2011).

Figures

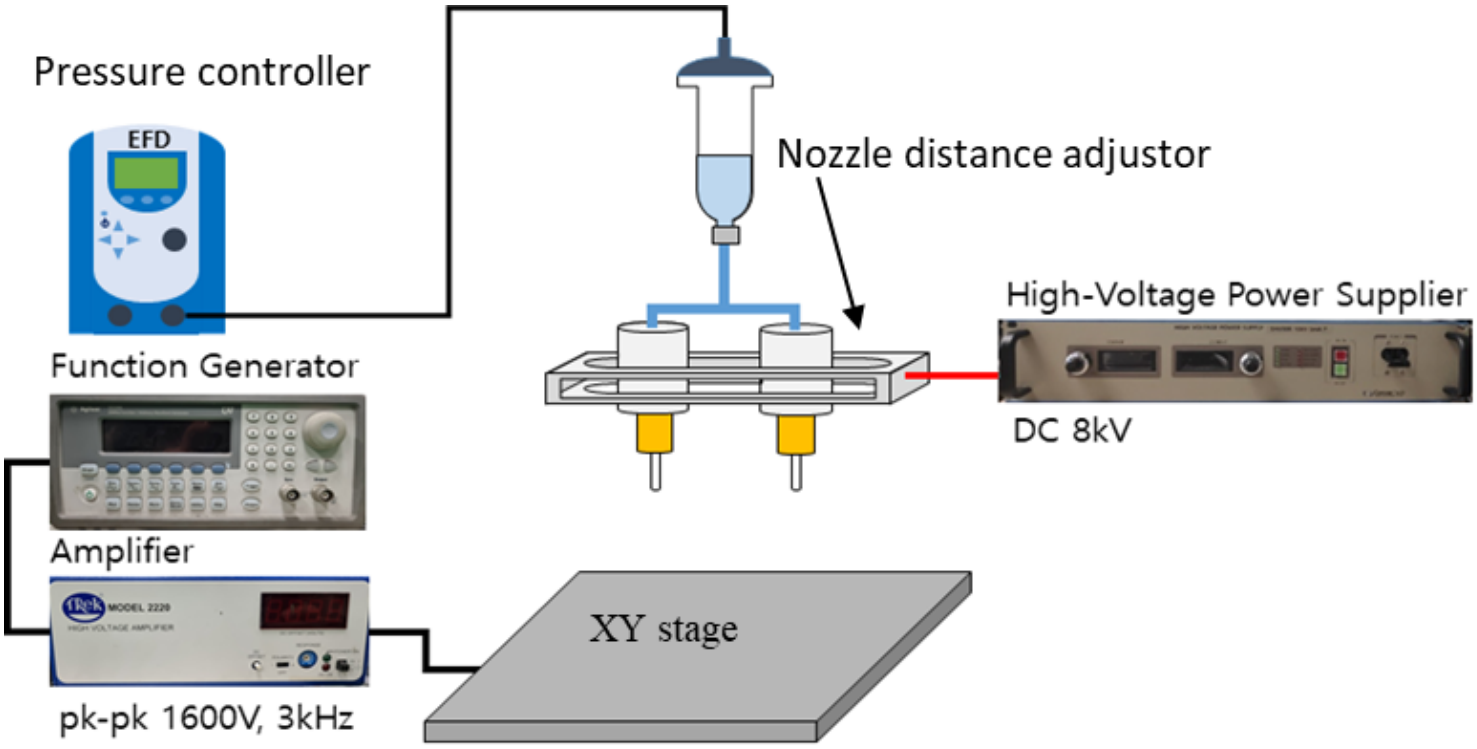

Figure 1

Schematic of investigation of the crosstalk effect between two nozzles.

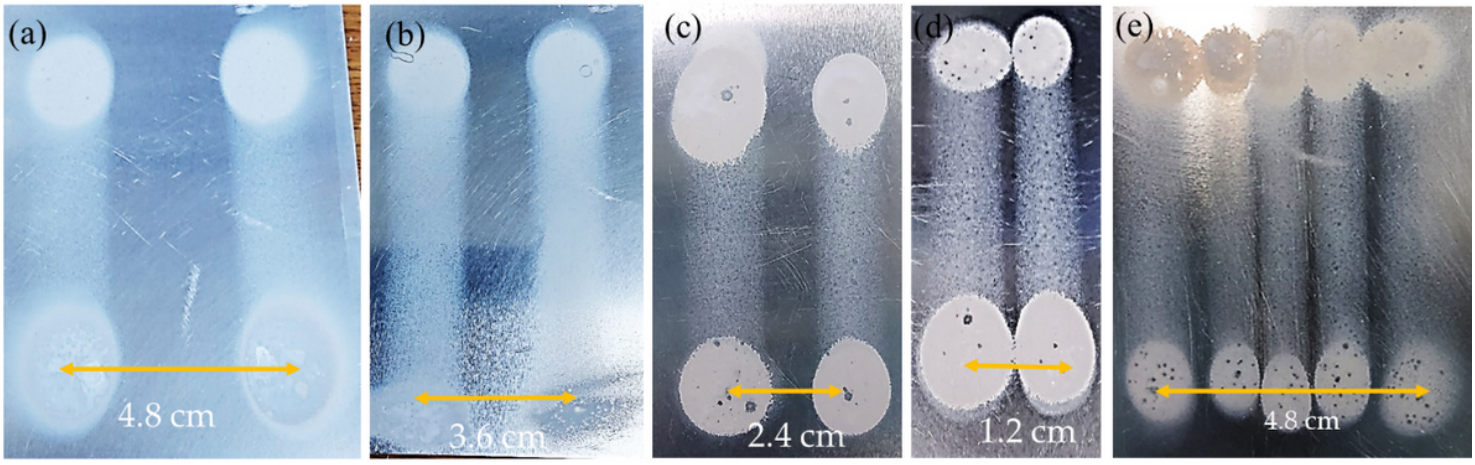

Figure 2

(a-d) Photo of electrospray depositions according to the distance between nozzles when two nozzles with an inner diameter of 330 μm are used (DC voltage of 8kV was applied at the nozzles and air pressure of 4 kPa was applied at the syringe barrel) and (e) Photo of deposited shapes using multi-head containing five nozzles with nozzle spacing of 1.2 cm.

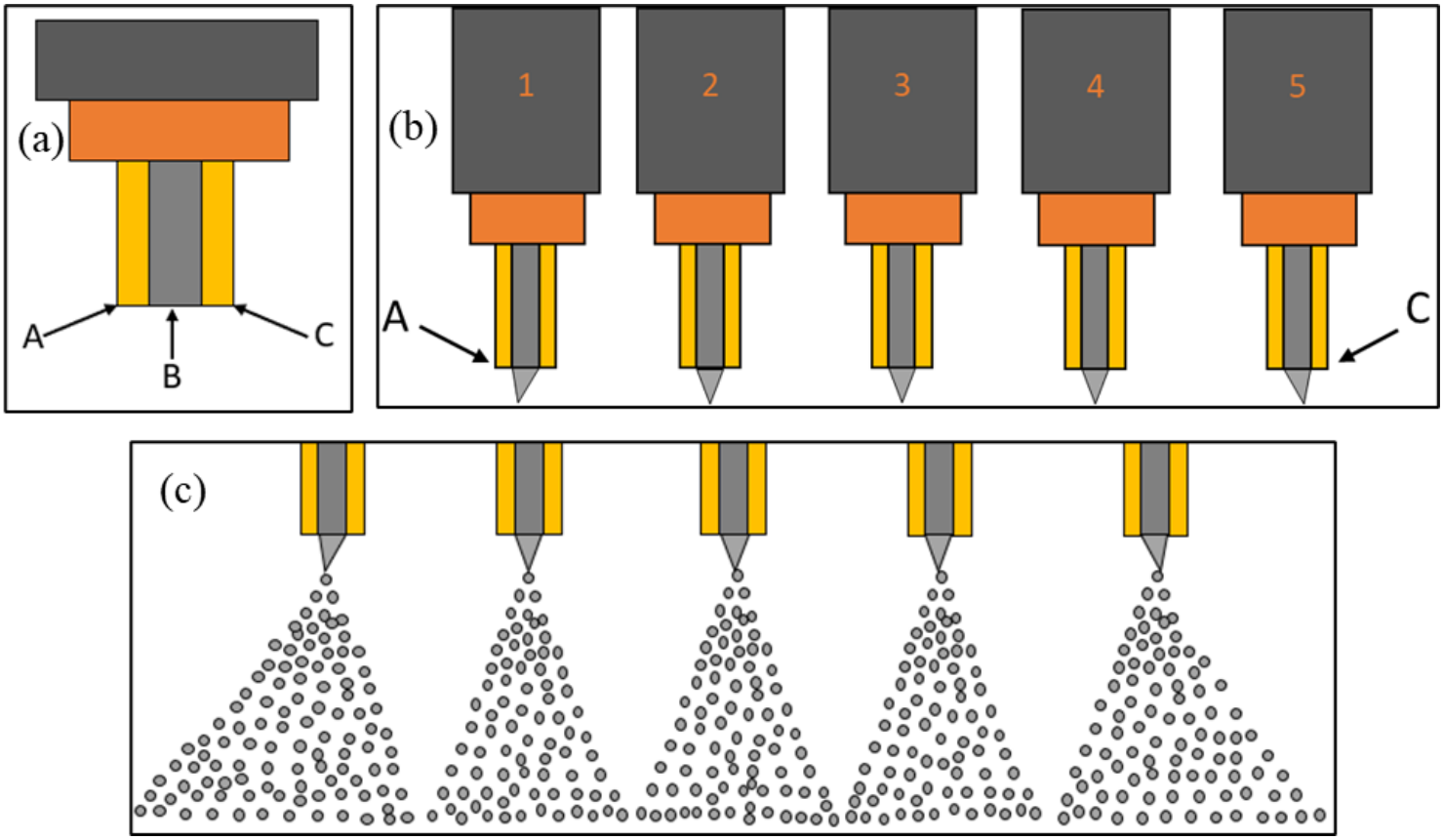

Figure 3

Illustration of different deposition behavior according to nozzle location: schematic of (a) different parts in a nozzle (A & C - two edge, B-middle part), (b) meniscus shape deformation at both ends of a linear array multi-nozzle spray head and (c) spray behaviors according to nozzle locations. The electric field at point A and C is not equal in case of end nozzle (nozzles 1 & 5). However, the electric field at A & C equals in middle nozzles (nozzles 2, 3 & 4).

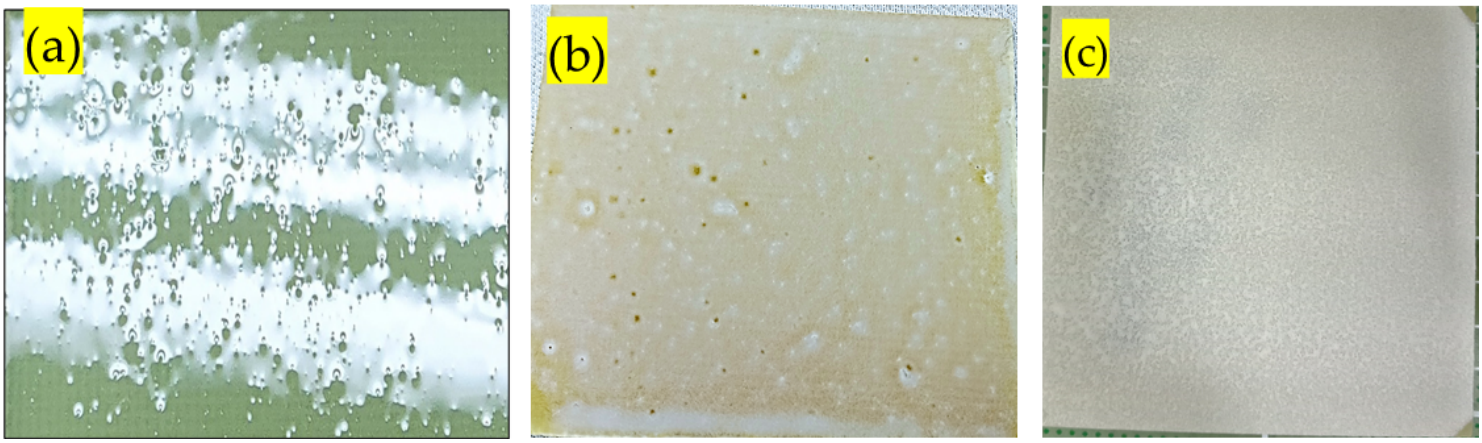

Figure 4

(a) Material agglomeration behavior of deposited materials on PCB substrate, (b) photo of non-uniform deposited layer taken after curing for 30 min at temperature 180 ˚C and (c) sprayed PCB surface with platen (substrate) heater on (100˚C) during deposition.

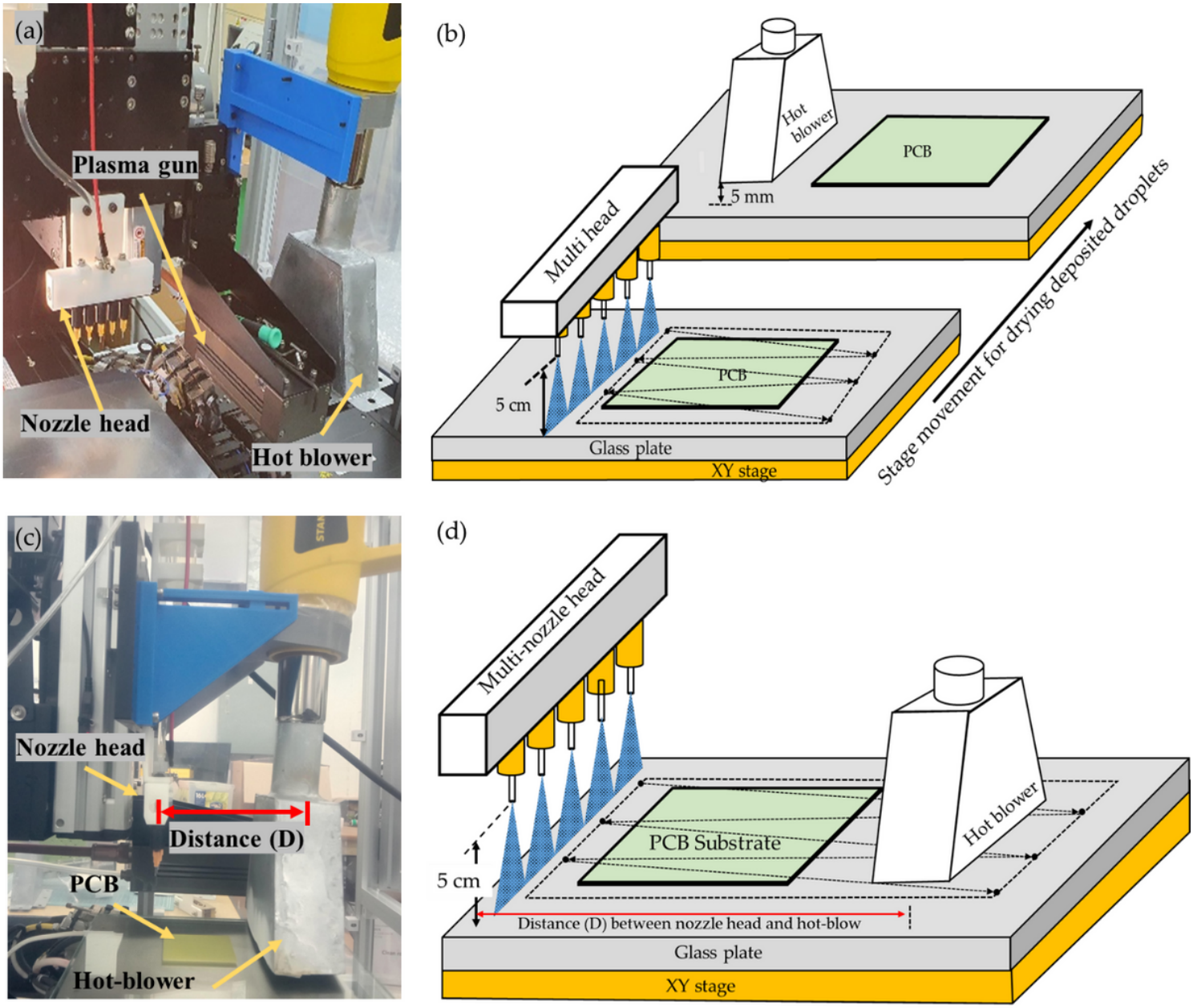

Figure 5

(a,b) Photo and schematic of the experimental setup for multi-nozzle spray head and drying unit (separately placed) with a time delay of the drying process and (c,d) photo and schematic of combined multi-nozzle spray head and drying unit with the fast and in-situ evaporation process.

(a)

Wind speed (m/s)	Hot blower temperature			
	50˚C	100˚C	150˚C	250˚C
1.5	Not dry	Not dry	Dry	Dry
3.6	Moderate dry	Moderate dry	Dry	Dry

(b)

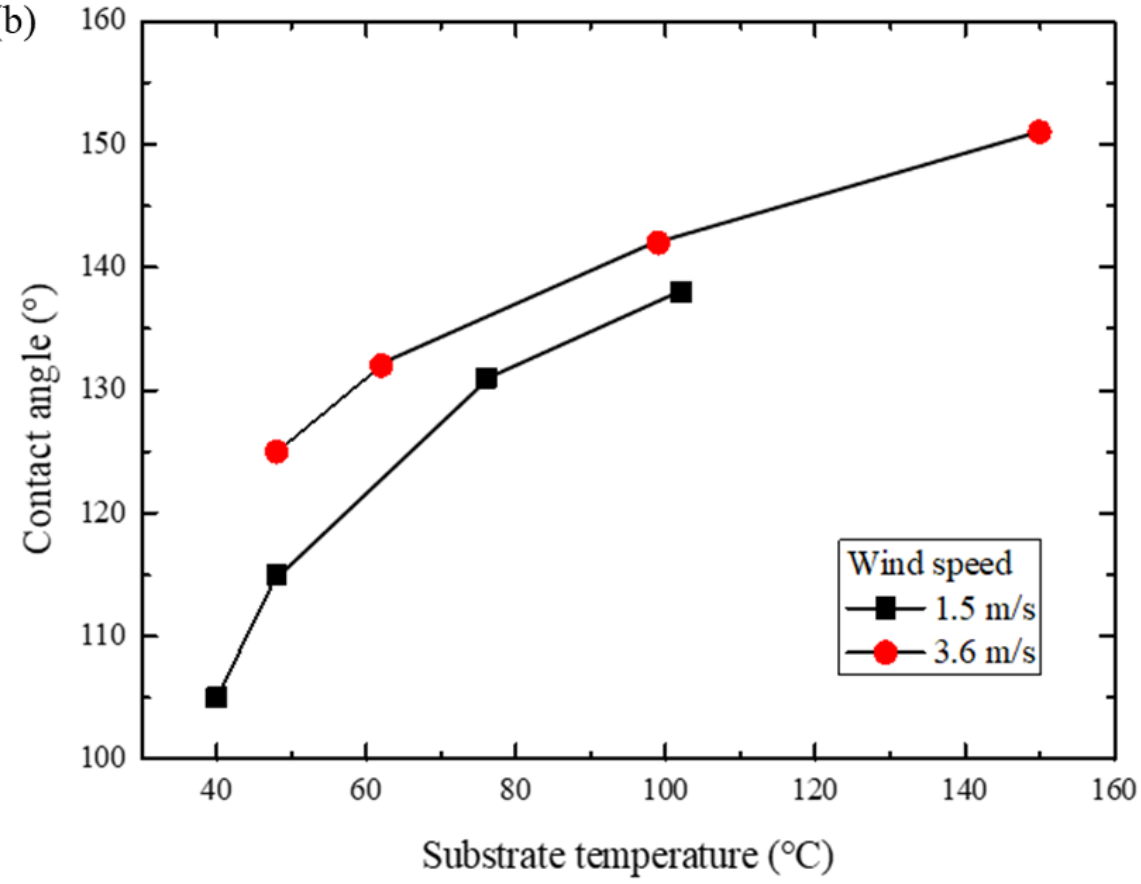

Figure 6

Drying effect using first configuration (spraying and drying separately): (a) Drying behavior of deposited materials on PCB substrate depending on hot blower temperature and wind speeds according (b) Water contact angle of deposited layers according to the substrate temperatures and wind speeds.

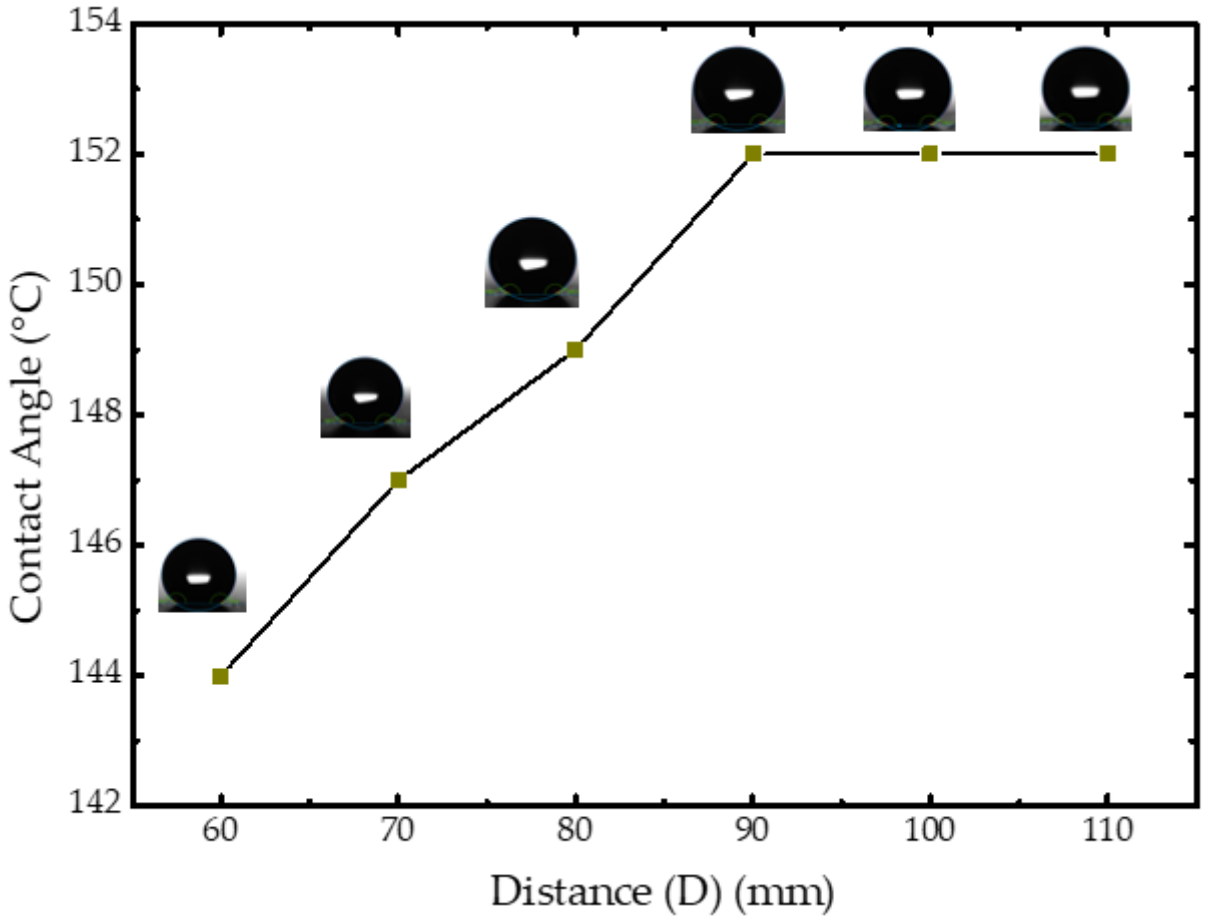

Figure 7

Contact angles of deposited layers according to distances between the hot blower and the nozzle head (Hot blower parameter: substrate temperature 150° and wind speed 3.6 m/s).

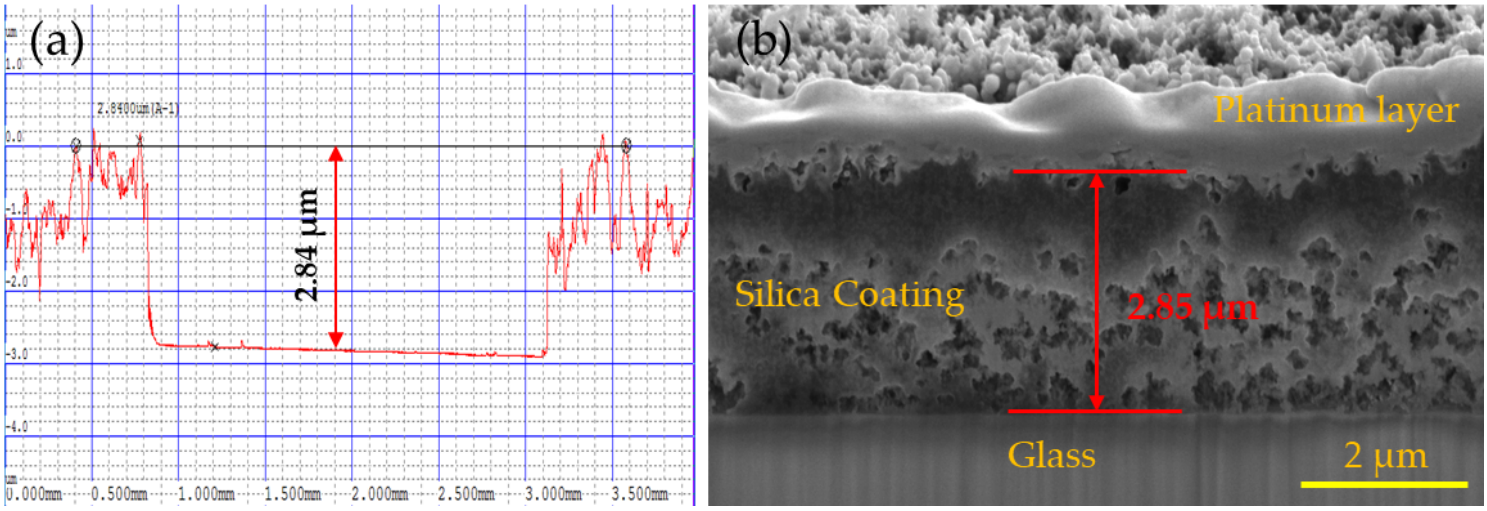

Figure 8

Thickness measurement of the coating layer on glass substrate: (a) 3- D profiler and (b) Cross-sectional FIB-SEM.

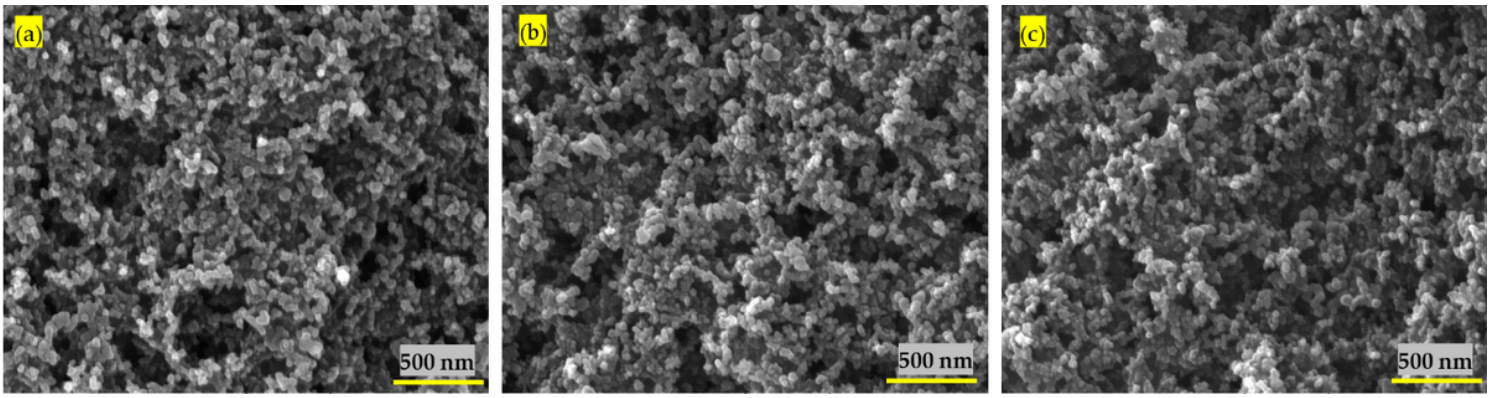

Figure 9

FE-SEM image; surface morphology of coated layers on PCB substrate: (a) before reliability test, (b) after sandpaper test and (c) after chemical test.

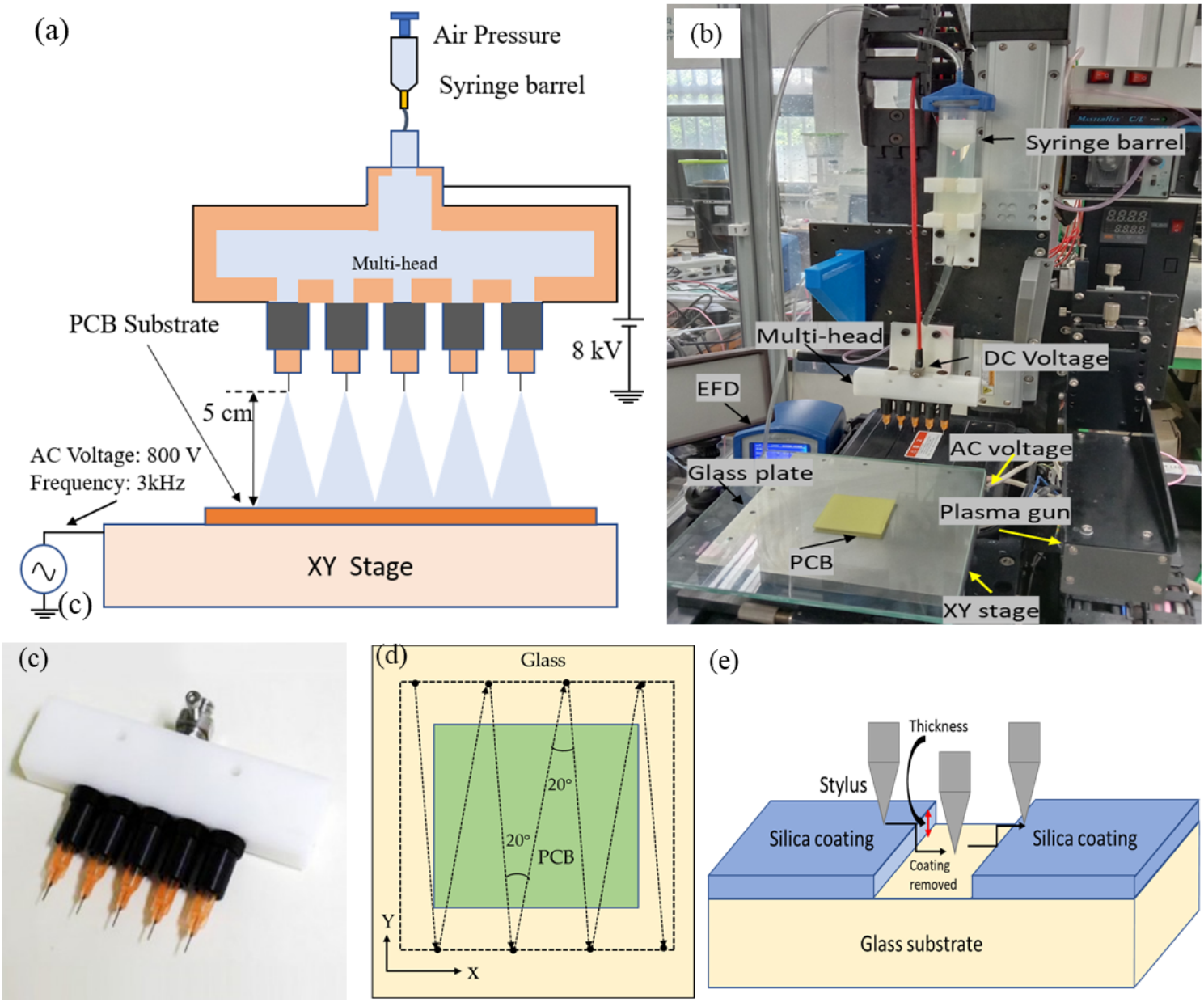

Figure 10

(a) Schematic of AC electrospray using multi-nozzle system, (b) experimental setup image, (c) multi-nozzle head (d) schematic of zig-zag printing and (e) schematic of the coated layer thickness measurement using 3D profiler.

Supplementary Files

This is a list of supplementary files associated with this preprint. Click to download.

- MovieS1.mp4
- MovieS2.mp4
- MovieS3.mp4

- MovieS4.mp4
- MovieS5.mp4
- MovieS6.mp4
- MovieS7.mp4
- Supplementaryinformationformultinozzleelectrosprayver5.docx